Electronics and Electrical Engineering

AIMS Electronics and Electrical Engineering, 6(3): 198–222.
DOI: 10.3934/electreng.2022013
Received: 07 February 2022
Revised: 16 June 2022
Accepted: 19 June 2022
Published: 11 July 2022

http://www.aimspress.com/journal/ElectrEng

Research article

Investigating the S-parameter ($|S_{11}|$) of CPW-fed antenna using four different dielectric substrate materials for RF multiband applications

Sandeep Kumar Singh[1,2,*], Tripurari Sharan[2] and Arvind Kumar Singh[2]

[1] Department of EECE, SET, Sharda University, Greater Noida, 201308, India
[2] North Eastern Regional Institute of Science and Technology, Nirjuli, 791109, India

*** Correspondence:** Email: sandeepsingh.ec@sharda.ac.in.

Abstract: This article aims to examine the $|S_{11}|$ parameter of a multiband Coplanar Waveguide (CPW)-fed antenna. The proposed square-shaped antenna-1 (Ant.1) and antenna-2 (Ant. 2) are primarily composed of three ground terminal stubs: Terminal-1 (T1), Terminal-2 (T2), and Terminal-3 (T3), all of which have an inverted L-shaped radiating patch. The proposed antennas' resonance frequencies (f_r) can be adjusted by the electrical dimension and length of the stub resonators, the dielectric constant (ε_r) of substrate materials, and their appropriate thicknesses. It will have an impact on their return loss ($|S_{11}|$), Impedance Bandwidth (IBW), radiation pattern, and antenna performance in terms of frequency characteristics, as demonstrated in this article. The proposed structure based on Flame-Retardant fiber glass epoxy (FR4) substrate covered a wideband frequency range from 1.5 to 3.2 GHz, (IBW = 1.7 GHz) and from 3.4 to 3.65 GHz (IBW = 0.25 GHz). The total IBW is 1.95 GHz, at $S_{11} \leq -10$ dB with three resonance frequencies of values f_{r1} = 1.75, f_{r2} = 2.65, and f_{r3} =3.50 GHz) for triple-band applications. The results are compared with the research work reported earlier. The proposed Ant.1 ensured, dual and triple band applications whereas the proposed Ant. 2 ensured dual, triple and quad bands applications with reasonable antennas' sizes similar to the earlier reported works. Furthermore, the impacts of various substrate materials as well as different lengths of multi-stub resonators on the operating bands and resonance frequency are thoroughly explored and analyzed for these antennas.

Keywords: coplanar waveguide; substrate material; radio frequency; multiband

1. Introduction

Owing to the significant prominence in current research on awareness of compact multi-band devices, design methods have been reliant on efficiently modifying and optimizing the antenna shape and its overall geometry. The antennas having small structure, planar geometry, lightweight, low cost, and particularly offering two or more frequency bands coverage are extremely needed for wireless applications. The multiband antennas with excellent radiation characteristics and large impedance bandwidth with desired radian pattern are required for advanced communication systems [1]. The best antenna that meets these requirements, is an antenna fed by a coplanar waveguide, since it provides low leakage of radiation and less dependence of characteristics impedance on substrate material and height. It is so because its patch, feed and ground are lying in the same plane which ascertains its easy integration with all other microwave devices.

In recent wireless communication systems, a multiband antenna has been playing a very important role in Radio Frequency (RF) service requirements. Personal Communications Service (PCS, 1.8/1.9 GHz), Digital Cellular System (DCS, 1.8 GHz), Global System for Mobile Communications (GSM, 1.8/1.9 GHz), International Mobile Telecommunication (IMT, 2.0/2.3/2.8/3.8/4.6 GHz), Universal Mobile Telecommunications System (UMTS, 2.1 GHz), Worldwide Interoperability for Microwave Access (WiMAX, 2.5/3.5/5.5 GHz), and Wireless Local Area Network (WLAN, 2.4/5.2/5.8 GHz) have been widely applied in mobile devices, such as handheld computers and intelligent phones [2–4]. The unique open-ended slots are used in a compact Asymmetric Coplanar Strip (ACS)-fed printed monopole antenna for WLAN and WiMAX applications. The slots are implanted in the ACS-fed monopole to bring two notched bands, as addressed in [2]. A CPW-fed triple-band planar monopole antenna is reported in [3]. Printed antenna structure over the rectangular substrate by cutting two rectangular corners of optimized size. The radiator of this antenna is very compact on which two Inverted-L-Shaped slots are etched to achieve three radiating elements to set three resonating modes for triple-band operation as addressed in [3]. A broadband asymmetric dual-loop antenna is reported [4] for wireless communication applications. This antenna consists of two asymmetric radiated loops and an asymmetric feeding structure, making it easy to offer combined effects of multiband, widened bandwidth with omni-directivity [4].

A compact triple-band microstrip slot antenna is suggested for multiband characteristics which are addressed in [5]. This antenna consists of a microstrip feed line, a substrate, and a ground plane on which some simple slots are etched. The rectangular and trapezoid slots can achieve dual frequencies and provide a broadband operation at high frequencies. The additional resonant mode is excited with the use of a pair of symmetrical horizontal strips embedded in the rectangular slot [5]. A planar geometry triple-band CPW-fed antenna is developed for wireless applications. The wide IBW performance of the antenna is ensured, by using different shapes of tuning stubs and modified ground plane structures, as reported in [6,7]. A rectangular multiband planar antenna with defected ground structure is demonstrated. T-shaped slits are introduced on either side of the radiating patch which offers a dual-band with better IBW. Further, a zig-zag shaped slit is inserted, due to which the antenna resonates at an additional third band, as described in [8]. The CPW-fed patch antenna designs are proposed for triple and quad-band applications with various shapes of structures. Slot loading methods are used to reduce the size of a patch antenna and to produce multiband operation in a stated frequency range, which is reported in [9–12].

Substrate material and slot techniques are used for size reduction and impedance matching, which is laminated on different dielectric materials for multiple communication systems as explained in [13–16]. The performance assessment of CPW-fed antenna using various substrate materials and

its thickness are introduced in [17–19]. A parametric study on three different high dielectric substrate materials for multiband and large impedance bandwidth characteristics is investigated in [20]. A novel method has been developed to reduce the size of the antenna without affecting other constraints of geometry. This is conceivable of different types of dielectric substrate material [20–23]. The performance of the antenna mainly depends on the properties of dielectric materials used in the antenna design and fabrication. The study of microwave materials and their dielectric properties at microwave frequencies is a precondition to selecting appropriate materials for numerous microwave applications [21]. The thicker substrate carries more efficiency and wider IBW with lower dielectric constant but large antenna size. Hence high dielectric constant substrate technique to allow overall appropriately small antenna size has been analyzed for RF and microwave applications [22,23].

In this article, compact square-shaped planer antennas (Ant.1 and Ant.2) have been proposed and designed for RF communication systems that can support multiband applications. Three ground terminal stubs, T1, T2, and T3, and an inverted L-shaped radiating stub are etched on a square-shaped patch for the proposed antennas. The suggested CPW-fed antenna's $|S_{11}|$ parameters have been evaluated. To accomplish the required performance characteristics for multiband operations, it is built utilizing four distinct dielectric materials with ε_r of 2.2, 3.2, 4.3, and 9.8.

The proposed Ant.1 is laminated on Alumina (ε_r = 9.8) to set two resonating modes for dual-band operation at f_{r1} = 1.9 GHz and f_{r2} = 2.8 GHz frequencies. Its wide bandwidth of 0.55 GHz at −15 dB (1.70-2.25 GHz) and 0.60 GHz at −20 dB (2.50-3.10 GHz) covers the GSM 1800/1900 (1.710-1.805 GHz and 1.850-1.990 GHz) and 2.8 GHz IMT (2.700-2.900 GHz) bands completely.

The proposed Ant.2 is based on FR4 (ε_r = 4.3) and Rogers (ε_r = 2.2) to cover three and four operating bands, respectively. Based on FR4 substrate Ant.2 (Q) resonates at f_{r1} = 1.75 GHz, f_{r2} = 2.65 GHz, and f_{r3} = 3.50 GHz frequencies, covering three different bandwidths of 0.25 GHz at −15 dB, 0.40 GHz at −20 dB, and 0.25 GHz at −10 dB, which can fulfil PCS 1.8/1.9 GHz (1.750-1.870 GHz and 1.880-1.990 GHz), and WiMAX 2.5/3.5 GHz (2.500-2.690 GHz and 3.400-3.690 GHz) bands.

The influences of substrate materials and lengths of multi-stub resonator on the operating bands and resonance frequencies have also been investigated in proposed Ant.2 (Q) based on Rogers substrate. The antenna resonates at 1.4/1.9/3.2/3.8 GHz and covers four separate impedance bandwidths of 0.25 GHz at −10 dB (1.35-1.60 GHz), 0.50 GHz at −12 dB (1.70-2.20 GHz), 0.75 GHz at −15 dB (2.75-3.50 GHz), and 0.55 GHz at −15 dB (3.60-4.15 GHz), which may satisfy IMT service (f_c = 1.4 GHz, FDD LTE band), GSM 1800/1900 (1.710-1.805 GHz and 1.850-1.990 GHz), Radio Location Service (f_c = 3.1 GHz) and IMT (f_c = 3.8 GHz, 3.400-4.200 GHz) bands.

Computer Simulation Technology (CST) implements the design and simulation results. The antenna design is performed using CST, the electromagnetic simulation software inside the microwave studio utilizing the Finite Integration Technique (FIT) in transient mode. The rest of the article is organized as follows. The antenna shape and substrate material are discussed in detail in section 2. The proposed antennas' design topology and improved $|S_{11}|$ parameters are discussed in section 3. The parametric studies being an important parameter are presented in section 4 for both the proposed antennas, and the article is concluded in section 5.

2. Antenna geometry and substrate materials

Figure 1 depicts the shape of the base antenna [17,18] and suggested CPW-fed square patch antennas, with geometrical characteristics listed in Table 1. The proposed Ant.1, Ant.2 (T), and Ant.2 (Q) are all designed on a FR4 substrate with a 0.76 mm thickness, ε_r = 4.3, loss tangent (tanδ) of

0.017, and overall dimensions of 50 (L) × 50 (W) mm^2. An inverted L-shaped radiator stub and ground planes with a thickness of 0.08 mm have been implanted on the upper layer of the substrate for all these antennas. To set the 50 Ω impedance, the CPW-fed line of the base antenna and proposed antenna is 4.2 mm wide (W_R) and has a gap distance (Gap) of 0.3 mm between the feed-line and the ground plane. The radiating patch has made up of an inverted L-shaped stub with a W_R = 4.2 mm and lengths of L_X and L_Y of 10.5 mm in both directions.

The resonance frequencies of an antenna are determined by the substrate's dielectric constant, thickness, and area of radiating stubs [13,14]. An antenna has been built to improve performance by selecting the appropriate substrate material and thickness [17–19]. There are a few technologies that can be used to increase the bandwidth of a CPW-fed antenna without changing its geometry.

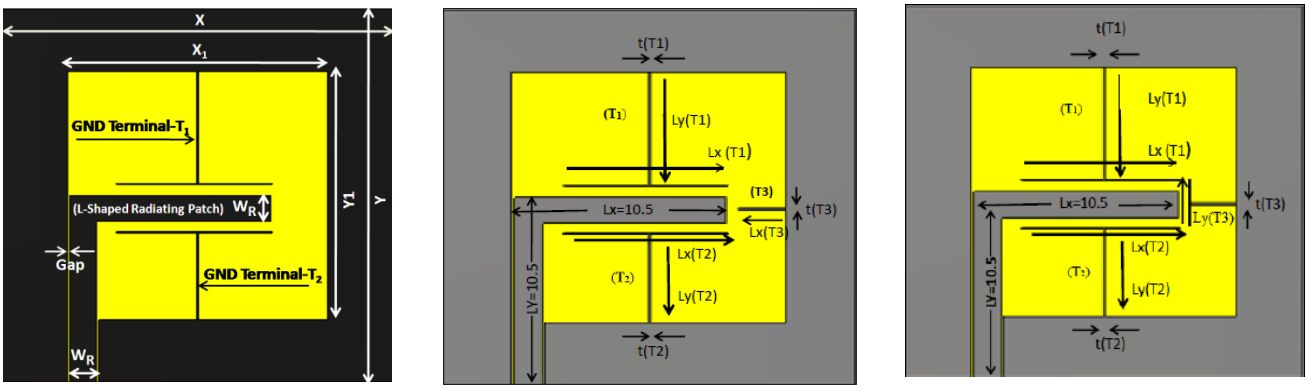

(a) (b) (c)

Figure 1. Front view geometry: (a) base antenna, (b) proposed Ant.1, and (c) proposed Ant.2.

Table 1. Optimized geometrical units of the base and proposed antennas.

Antennas	Schematic Configuration of Proposed Antennas (Units: mm)									
	Ground Terminal-1 (T1)			Ground Terminal-2 (T2)			Ground Terminal-3 (T3)			Antenna Response
	Lx(T1)	Ly(T1)	t(T1)	Lx(T2)	Ly(T2)	t(T2)	Lx(T3)	Ly(T3)	t(T3)	
Base Ant. [17]	24.0	18	0.4	24.0	14	0.4	NA	NA	NA	Single-band
Base Ant. [18]	21.5	14.7	4.2	21.5	14.7	4.2	NA	NA	NA	Single-band
Proposed Ant.1	20.5	19	0.5	20.5	15	0.5	05	NA	0.5	Dual-band
Proposed Ant.2 (T)	20.5	19	0.5	20.5	15	0.5	07	8	0.5	Triple-band
Proposed Ant.2 (Q)	20.5	19	0.5	20.5	15	0.5	07	16	0.5	Triple/Quad band
Lx: Length in x-direction: Ly: Length in y-direction: Lx(T1): Length of terminal-1 in x-direction; Lx(T2): Length of terminal-2 in x-direction; Lx(T3): Length of terminal-3 in x-direction; Ly(T1): Length of terminal-1 in y-direction; Ly(T2): Length of terminal-2 in y-direction; Ly(T3): Length of terminal-3 in y-direction; t(T1): Width thickness of terminal-1; t(T2): Width thickness of terminal-2; t(T3): Width thickness of terminal-3; (T): Triple-band; (Q): Quad-band; NA: Not Applicable										

The soft substrate offers low value of dissipation factor as compared to hard substrate, so the prior is preferred for the design of microstrip patch antenna. However, owing to its poor dimensional stability, soft substrate-based antenna, relatively offers limitation at higher frequency ends. Its dielectric constant variation further, limits the upper usable frequency range. They are available as a single layer of metallization supporting micro-strip construction and some have thick metal backing,

which assists in mechanical stability and heat removal. Soft substrates are available for microwave applications up to a few GHz and have fine fiber weaves [20–22]. There are a few examples of soft substrates that can be used at frequencies well above 10 GHz and are listed in Table 2.

The application of different soft substrates material having a dielectric constant ranging from $2.2 \leq \varepsilon_r \leq 12$ provides higher bandwidth. If the substrate material of a CPW-fed patch antenna is changed, the overall antenna performance is affected. The selection of proper substrate material plays a vital role in antenna design [17]. Several researchers used $\varepsilon_r > 2.2$ for specific purposes such as higher IBW, more gain, etc. The proposed Ant.1 and Ant.2 are made from four different substrate materials with dielectric constants of 2.2 (Rogers), 3.2 (Arlon), 4.3 (FR4 Epoxy), and 9.8 (Alumina). As shown in Table 7, the substrate thicknesses of 1.11 mm, 0.95 mm, 0.76 mm, 0.51 mm, and 0.40 mm are examined for each substrate material.

Table 2. Properties of typical microwave substrate materials.

Property	Rogers	Arlon	FR4	Alumina	Condition/Range
Dielectric Constant (ε_r)	2.2	3.2	4.3	9.8	1 to 10 GHz
Dissipation Factor (tanδ)	0.0004	0.0038	0.017	0.0020	10 GHz
Thermal Coefficient of ε_r (ppm/ ℃)	−125	−110	−80	−43	−55 to +125 ℃
Thermal Conductivity (W/m.K)	0.26	0.235	0.45	0.76	80 to 100 ℃
Specific Heat (J/g.K)	0.96	0.90	0.95	0.72	-
Volume Resistivity (MΩ-cm)	$2x10^7$	$1.2x10^9$	$8x10^7$	$2x10^8$	-
Surface Resistivity (MΩ)	$3x10^7$	$4.5x10^7$	$2x10^5$	$4x10^7$	-
Break down voltage (kV)	>60	>45	>32	>18	-
Moisture Absorption (%)	0.02	0.06	0.25	0.16	-

3. Optimization of ground terminals for $|S_{11}|$ parameter

In this section, the $|S_{11}|$ parameters of the base and proposed antennas with various configurations were simulated and the results are analyzed. Figure 2 shows the optimal $|S_{11}|$ parameter for the base antennas at a single resonance frequency [17,18]. Figure 2 shows the $|S_{11}|$ parameter resonating at f_{r1}= 2.8 GHz for the reference antenna [17] and f_{r1} = 2.4 GHz for the reference Type-II antenna [18] for single-band application. The authors S. K. Singh et al. have addressed a CPW fed antenna which uses the resonator stub of the variable length and provides a wider IBW of 1.7 GHz (1.4–3.1 GHz) at −10 dB [17].

The proposed Ant.1 has resonance frequencies of f_{r1} = 2.1 GHz and f_{r2} = 2.8 GHz at Lx(T3) = 5 mm, as well as wide IBW 0.35 GHz (1.9-2.25 GHz) at −18 dB and 0.55 GHz (2.5-3.05 GHz) at −20 dB for dual-band applications, as shown in Figure 3. The effect of changing the geometrical unit, such as increasing the resonator path length of Lx(T3) from 1 mm to 7 mm $\{1 \leq Lx(T3) \leq 7\}$ of the ground terminal (T3) leads to a modest shift in the resonance frequencies towards the low-frequency band seen in Figure 3.

Figure 4 depicts the S parameter of Ant.2 useable in triple-band applications with a constant stub length Lx(T3) = 7 mm and a variable stub length Ly(T3) ranging from 8 to 20 mm. The predicted resonance frequencies of Ant. 2 for Ly(T3) = 8 mm are f_{r1} = 1.25 GHz, f_{r2} = 1.8 GHz, and f_{r3} = 2.8 GHz, which fall in the low-frequency ranges. The resonance frequencies of the proposed Ant.

2 at Ly (T3) = 16 mm are f_{r1} = 1.65 GHz, f_{r2} = 2.6 GHz, and f_{r3} = 3.5 GHz, all of which are in the high-frequency ranges. The bandwidths are 0.25 GHz (f_{r1} = 1.65 GHz, 1.60-1.85 GHz) at −14 dB, 0.75 GHz (f_{r2} = 2.6 GHz, 2.10-2.85 GHz) at −15 dB, and 0.30 GHz (f_{r3} = 3.5 GHz, 3.35-3.65 GHz) at −10 dB for triple-band applications. The optimal $|S_{11}|$ parameter of proposed antennas, as well as the base antenna, is demonstrated in Figures 2, 3, and 4. The findings revealed a wide range of IBW for antennas with different resonance frequencies.

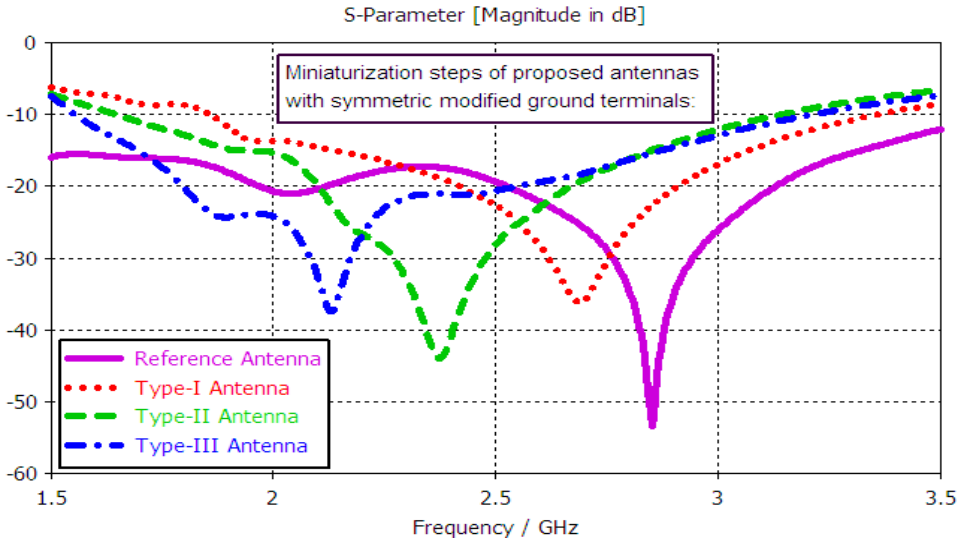

Figure 2. $|S_{11}|$ variation of base antenna for the single-band application**.**

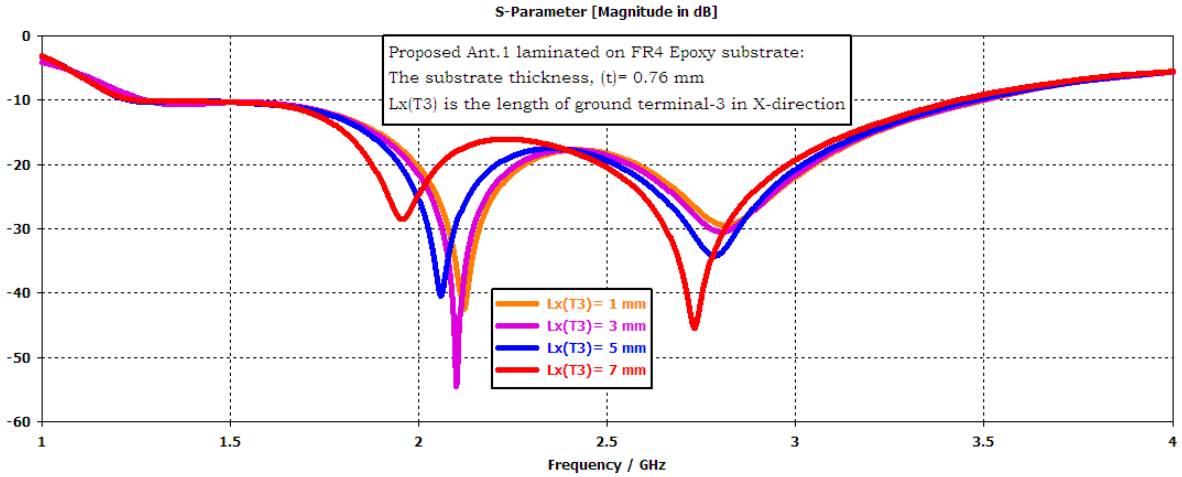

Figure 3. $|S_{11}|$ variation of proposed Ant.1 for dual-band applications.

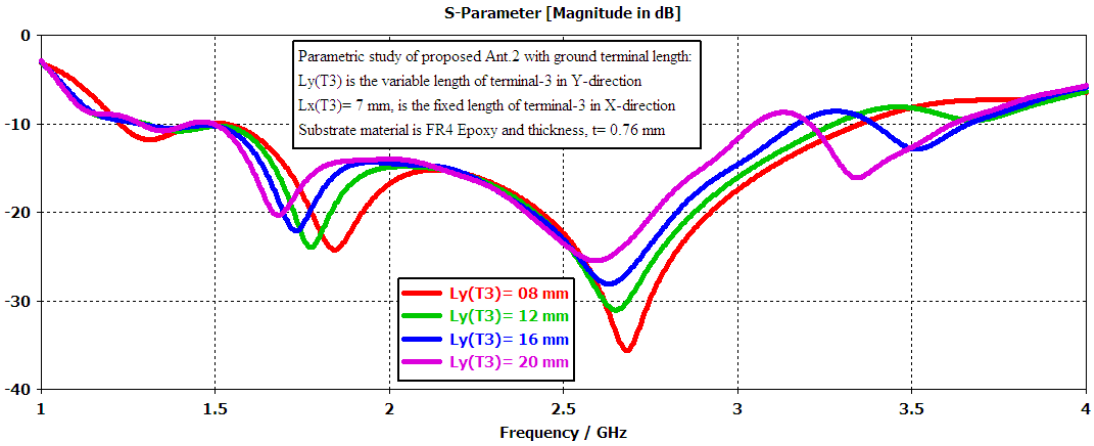

Figure 4. $|S_{11}|$ variation of proposed Ant.2 for triple-band applications.

3.1. Design procedure of the proposed antenna-1

The four different geometrical configurations of the antenna composed of Step-1, Step-2, Step-3, and Step-4 are shown in Figure 5(a–d), respectively with multi-stubs loaded ground terminal resonator [24,25]. These proposed antennas contain an inverted L-shaped radiating stub, and three asymmetrical ground terminal stubs resonator T1, T2, and T3 on the XY-plane of the FR4 substrate as shown in Figure 1(b) and Figure 1(c). In step-1, the terminal length of the resonator in the x-direction is Lx(T3) and the width thickness is 0.5 mm {tw(T3)} of ground terminal-3, which has been optimized with resonant path length L_{33} {Lx(T3)}, as shown in Figure 5(a). The structure of step-2 uses resonant path length L_{11} {Lx(T1) + Ly(T1) + Lx(T3)} with fixed width thickness tw(T1) of 0.5 mm as shown in Figure 5(b). In step-3 the antenna is simulated with resonant path length L_{22} {Lx(T2) + Ly(T2) + Lx(T3)} as shown in Figure 5(c). The design evolution step-4 of proposed Ant.1 having three ground terminal stubs are set to the total length of the resonator L_{34} {Lx(T1) + Ly(T1) + Lx(T2) + Ly(T2) + Lx(T3)} as shown in Figure 5(d). The various geometrical design parameter units {1 mm ≤ Lx(T3) ≤ 7mm} of the proposed Ant.1 are optimized using the CST as tabulated in Table 1 and illustrated in Figure 3 for dual notch-band frequency applications. Thus, the design approach for the excitation of resonance frequencies is due to the length of individual stub resonators.

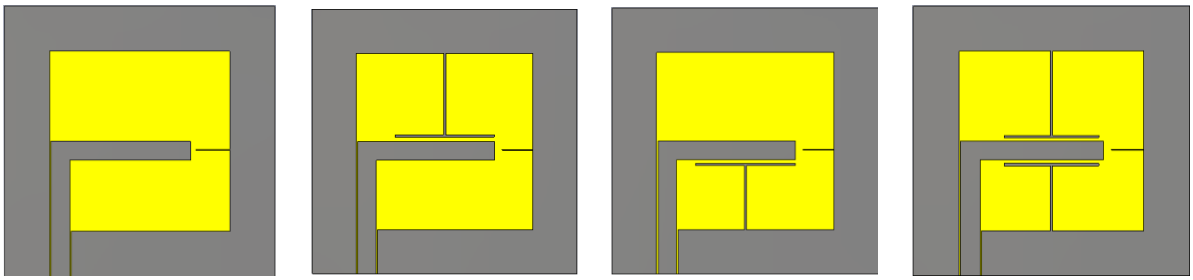

Figure 5. Step by step evolution of proposed Ant.1 with multi-stubs loaded resonator; (a) Step-1: Single ground terminal antenna (T_3), (b) Step-2: Double ground terminal antenna (T_1 and T_3), (c) Step-3: Double ground terminal antenna (T_2 and T_3), and (d) Step-4: Proposed Ant.1 with Triple ground terminal (T_1, T_2, and T_3).

3.2. Design procedure of the proposed antenna-2

Figure 6 shows the different lengths of the stub resonator for the design evolution of the proposed Ant. 2 with four geometrical configurations of ground terminal-3. The resonator path length of terminal-3 stub in y-direction {Ly(T3)} is varied from 8 mm ≤ Ly(T3) ≤ 20 mm for the excitation of multi resonance mode [24,25]. Its different geometrical units are tabulated in Table 1, and structures are illustrated in Figure 6(a–d).

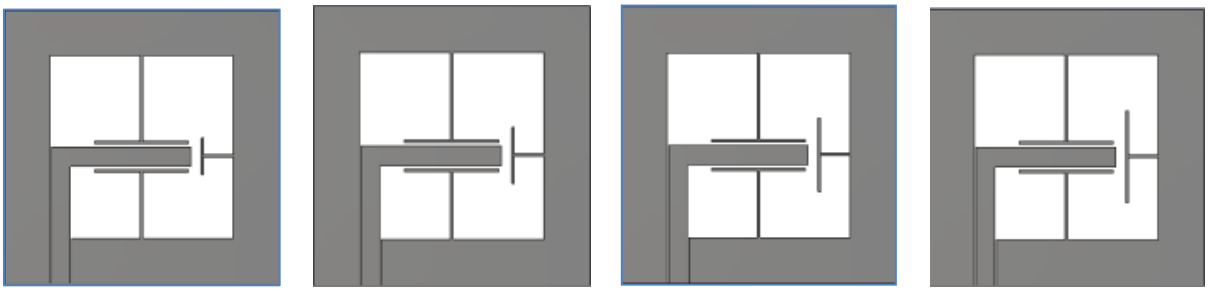

Figure 6. Step by step evolution of proposed Ant.2; (a) Step-1: Ly(T3) = 8 mm, (b) Step-2: Ly(T3) = 12 mm, (c) Step-3: Ly(T3) = 16 mm, and (d) Step-4: Ly(T3) = 20 mm.

The $|S_{11}|$ parameters of the proposed Ant. 2 are optimized at Ly(T3) = 8 mm, 12 mm, 16 mm, and 20 mm. The proposed Ant. 2 has three ground terminal stubs which are used to set the total resonant path length L_{44} {Lx(T1) + Ly(T1) + Lx(T2) + Ly(T2) + Lx(T3) + Ly(T3)} intended for their three resonant frequencies (f_r) which are shown in Figure 4 for triple-band applications. Thus, a parametric study has been carried out with FR4 substrate to get the optimal $|S_{11}|$ parameter for the proposed Ant.1 and Ant. 2 which is theoretically justified in section 4.

4. Parametric study of the proposed antennas

The parametric study is important for achieving appropriate impedance matching of the antenna and design parameters. The length of ground terminal stub resonators is widely considered during the design of the antenna to achieve the number of resonance frequencies and bands of CPW-fed antenna. Resonance frequencies and bands can be controlled by changing the length of ground terminal stubs as per the requirement of users [8,12,24]. The total length of ground terminal stub (L_{GTS}) resonators L_{33}, L_{11}, L_{22}, L_{34}, and L_{44} are used to determine the number of resonance frequencies (f_{rN}) by using equation (1).

$$f_{rN} = \frac{c}{2L_{GTS}\sqrt{\varepsilon_{reff}}} \tag{1}$$

where N is the number of resonating frequencies, L_{GTS} is the resonator path length, ε_{eff} is the effective dielectric constant, and c is the speed of light.

4.1. Effect of ground terminal stub lengths on $|S_{11}|$ parameter

The proposed Ant.1 and proposed Ant.2 have square-shaped geometry of the same size as an

inverted L-shaped radiating stub and the same substrate dimension of 50 mm (W) × 50 mm (L). The parametric study based on the asymmetrical ground terminals T1, T2, and T3 structures are shown in Figure 5 and Figure 6 for Ant.1 and Ant.2, respectively.

4.1.1. Length variation of L_{33}

The effects of the resonant path length (L_{33}) on the return loss $|S_{11}|$ of proposed Ant.1 (Step 1) are shown in Figure 7. The fundamental resonance frequency (f_{r1}) can be calculated using equation (2). As the length L_{33} increases, the magnitude of the $|S_{11}|$ parameter changes from −25 to −19 dB.

$$f_{r1} = \frac{c}{2L_{33}\sqrt{\varepsilon_{reff}}} \tag{2}$$

The length of stub L_{33} {Lx(T3)} changes from 4 mm ≤ Lx(T3) ≤ 8 mm, the resonance frequency (f_{r1}) is 2.8 GHz approximately to the entire range from 4 mm to 8 mm for the single-band operation. The variation of the $|S_{11}|$ parameter of the Ant.1 for step-1 is illustrated in Figure 7.

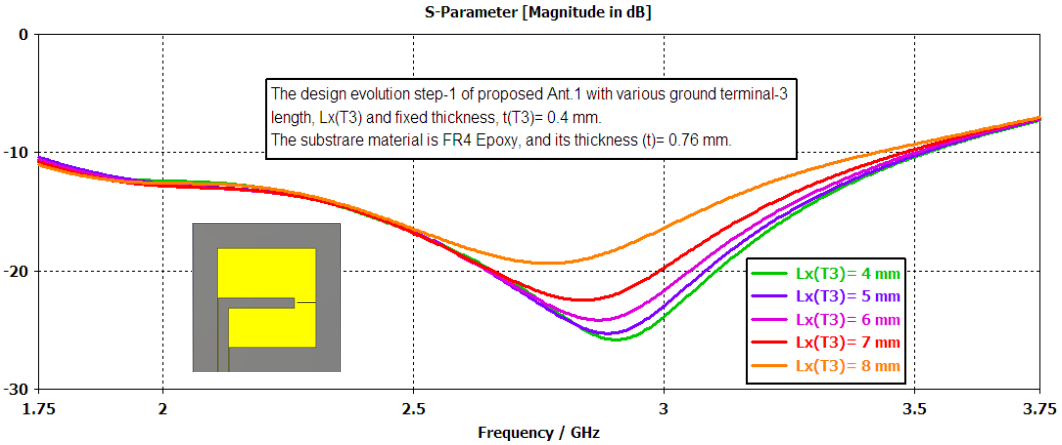

Figure 7. $|S_{11}|$ of proposed Ant.1 with Step-1; 4 mm ≤ Lx(T3) ≤ 8 mm.

4.1.2. Length variation of L_{11}

The effects of the resonant path length (L_{11}) on the return loss $|S_{11}|$ of the proposed Ant.1 (Step2) are shown in Figure 8. The total length of L_{11} {Lx(T1) + Ly(T1) + Lx(T3)} is varied with the help of ground terminal-1 {Lx(T1)}. Lx(T1) changed from 18.50 mm ≤ Lx(T1) ≤ 22.50 mm. The resonance frequencies ($f_{r1,\,2}$) are estimated by equation (3).

$$f_{r1,2} = \frac{c}{2L_{11}\sqrt{\varepsilon_{reff}}} \tag{3}$$

The stability of magnitude of $|S_{11}|$ increases as the length Lx (T1) is increased. The two resonance frequencies are found for dual-band application f_{r1} = 1.8 GHz and f_{r2} = 2.75 GHz for the first and second bands. The resonance frequency f_{r2} of the second band has a higher magnitude ($|S_{11}|$) as compared to the f_{r1} resonance frequency of the first band. The variation of the return loss of the Step-2 antenna is shown in Figure 8, the length of the ground terminal-1 stub optimized at Lx(T1) = 18.50 mm, 19.50 mm, 20.50 mm, 21.50 mm, and 22.50 mm, with fixed Ly(T1) and Lx(T3) geometrical parameters.

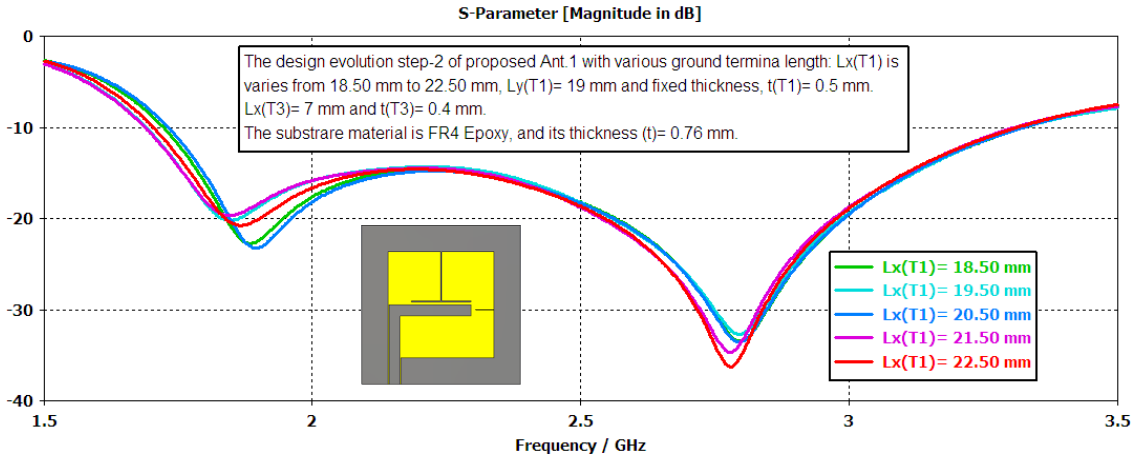

Figure 8. $|S_{11}|$ of proposed Ant.1 with Step-2; 18.50 mm ≤ Lx(T1) ≤ 22.50 mm.

4.1.3. Length variation of L_{22}

The length of the ground terminal-2 {Lx(T2)} stub is varied to analyze the characteristics of proposed Ant.1 (Step 3). The total length of L_{22} = {Lx(T2) + Ly(T2) + Lx(T3)} is used to enhance the $|S_{11}|$ by using equation (4). The $|S_{11}|$ characteristics with the ground stub Lx(T2) variation (18.50 mm ≤ Lx(T2) ≤ 22.50 mm) are shown in Figure 9.

$$f_{r1,2} = \frac{c}{2L_{22}\sqrt{\varepsilon_{reff}}} \tag{4}$$

The magnitude of $|S_{11}|$ increases as the stub length of the ground terminal Lx(T2) is raised from 19.50 mm to 20.50 mm, according to the analysis. Further, an increase in Lx(T2) to 21.50 mm, causes a decrease in the magnitude of $|S_{11}|$. The significant change in resonant frequencies f_{r1} and f_{r2}, also occur for both the first and second bands. The result proves that Lx(T2) = 22.50 mm produces wide IBW with a maximum magnitude of $|S_{11}|$.

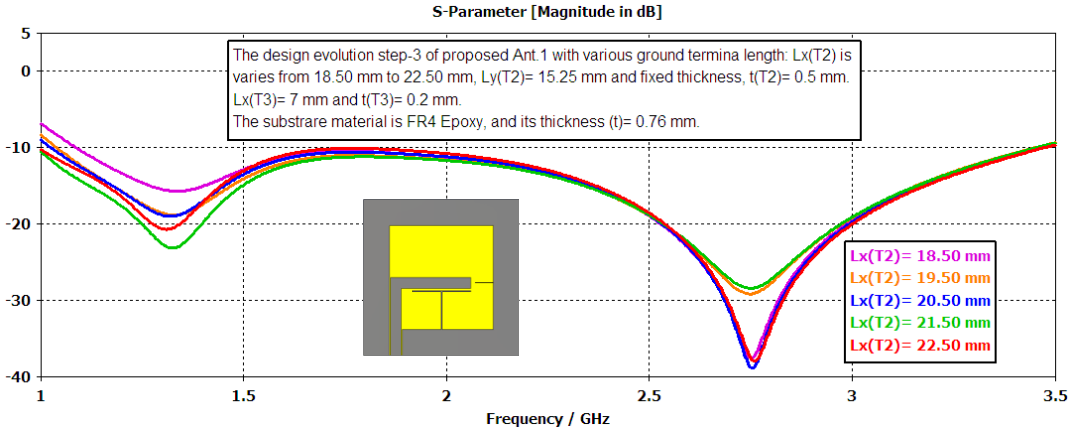

Figure 9. $|S_{11}|$ of proposed Ant.1 with Step-3; 18.50 mm ≤ Lx(T2) ≤ 22.50 mm.

4.1.4. Length variation of L_{34}

The optimal length of the Lx(T3) stub with two other ground terminals T1 and T2 can be used for the best $|S_{11}|$ characteristics of the proposed Ant. 1 (step 4). The variation in the length of ground T3 {1 mm ≤ Lx(T3) ≤ 7 mm} stub with the total length of L_{34} {Lx(T1) + Ly(T1) + Lx(T2) + Ly(T2) + Lx(T3)} is used to improve the $|S_{11}|$ characteristic by using equation (5).

$$f_{r1,2} = \frac{c}{2L_{34}\sqrt{\varepsilon_{reff}}} \tag{5}$$

The effect of different values of Lx(T3) on $|S_{11}|$ characteristics of the proposed Ant. 1 is illustrated in Figure 10. When the length of stub Lx(T3) is taken 5 mm, the antenna produces appropriate resonance frequencies f_{r1} and f_{r2} which are close to each other at 2.1 GHz (−40 dB) and 2.8 GHz (−35 dB), as shown in Figure 10. At Lx(T3) = 3 mm, $|S_{11}|$ covers a wide range of IBW with two resonance frequencies f_{r1} at 2.1 GHz (−55 dB) and f_{r2} at 2.85 GHz (−30 dB). The magnitude ($|S_{11}|$) of f_{r1} is higher as compared to f_{r2}. Similarly, at Lx(T3) = 7 mm, the resonance frequencies f_{r1} at 1.9 GHz (−28 dB) and f_{r2} at 2.75 GHz (−45 dB), in this case, the magnitude ($|S_{11}|$) of f_{r1} is lower as compared to f_{r2} as illustrated in Figure 10.

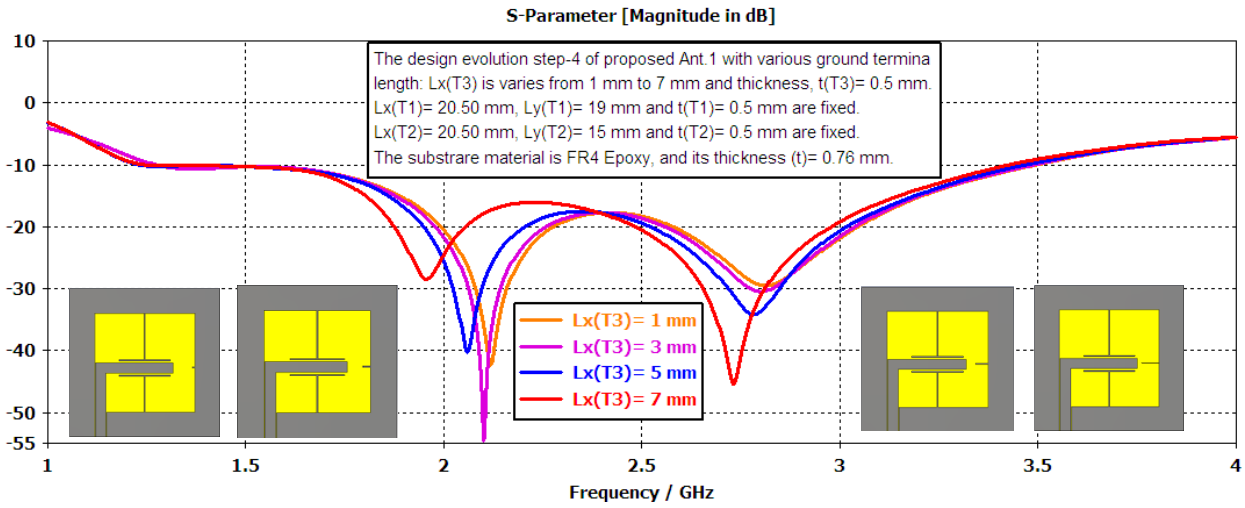

Figure 10. $|S_{11}|$ of proposed Ant.1 with Step-4; 1 mm ≤ Lx(T3) ≤ 7 mm.

When the stub length Lx(T3) is raised from 1mm to 7 mm for the proposed Ant.1, the resonance frequencies shift to the low-frequency regions. Table 3 shows that the antenna offers the optimal magnitude ($|S_{11}|$) for the suggested Ant.1 when Lx(T3) = 5 mm and Lx(T1) = Lx(T2) = 20.50 mm.

Table 3. Optimal resonance frequencies of proposed Ant.1 with different configurations.

Design Steps of Ant.1	Various Length of Ground Terminal Stubs and Substrate Thickness (t)						Resonance Frequencies (f_{rN}), (N = 1, 2)			
	Lx(T1) (mm)	Ly(T1) (mm)	Lx(T2) (mm)	Ly(T2) (mm)	Lx(T3) (mm)	FR4 (t) (mm)	f_{r1} (GHz)	$\|S_{11}\|_1$ (−dB)	f_{r2} (GHz)	$\|S_{11}\|_2$ (−dB)
Step-1	-	-	-	-	4	0.76	2.90	20	-	-
	-	-	-	-	5	0.76	2.90	21	-	-
	-	-	-	-	6	0.76	2.85	22	-	-
	-	-	-	-	7	0.76	2.85	23	-	-
	-	-	-	-	8	0.76	2.80	23	-	-
Step-2	18.50	19	-	-	7	0.76	1.90	20	2.85	34
	19.50	19	-	-	7	0.76	1.75	20	2.85	34
	20.50	19	-	-	7	0.76	1.90	20	2.85	34
	21.50	19	-	-	7	0.76	1.75	23	2.80	35
	22.50	19	-	-	7	0.76	1.80	23	2.80	36
Step-3	-	-	18.50	15.25	7	0.76	1.40	16	2.75	29
	-	-	19.50	15.25	7	0.76	1.35	19	2.75	30
	-	-	20.50	15.25	7	0.76	1.35	19	2.75	39
	-	-	21.50	15.25	7	0.76	1.35	20	2.75	39
	-	-	22.50	15.25	7	0.76	1.40	22	2.75	39
Step-4	20.50	19	20.50	15	1	0.76	2.10	45	2.85	30
	20.50	19	20.50	15	3	0.76	2.10	55	2.85	30
	20.50	19	20.50	15	5	0.76	2.05	40	2.80	32
	20.50	19	20.50	15	7	0.76	1.90	30	2.75	45

4.1.5. Length variation of L_{44}

The influence of ground terminal stub Ly(T3) as a resonator on the f_{rN} and IBW characteristics [24,25] is investigated by using equation (6). The resonant length Ly(T3) is varied from 8 mm to 20 mm, while the remaining two parameters (T1 and T2) are fixed. The effect of total resonant length (L_{44}) on $|S_{11}|$ for proposed Ant.2 has been illustrated in Figure 11 and tabulated in Table 4.

$$f_{r1,2,3} = \frac{c}{2L_{44}\sqrt{\varepsilon_{reff}}} \tag{6}$$

The findings in Table 4 show that the optimal magnitude of the $|S_{11}|$ parameter for the proposed Ant.2 is set for Lx(T3) = 16 mm and Lx (T1) = Lx(T2) = 20.50 mm.

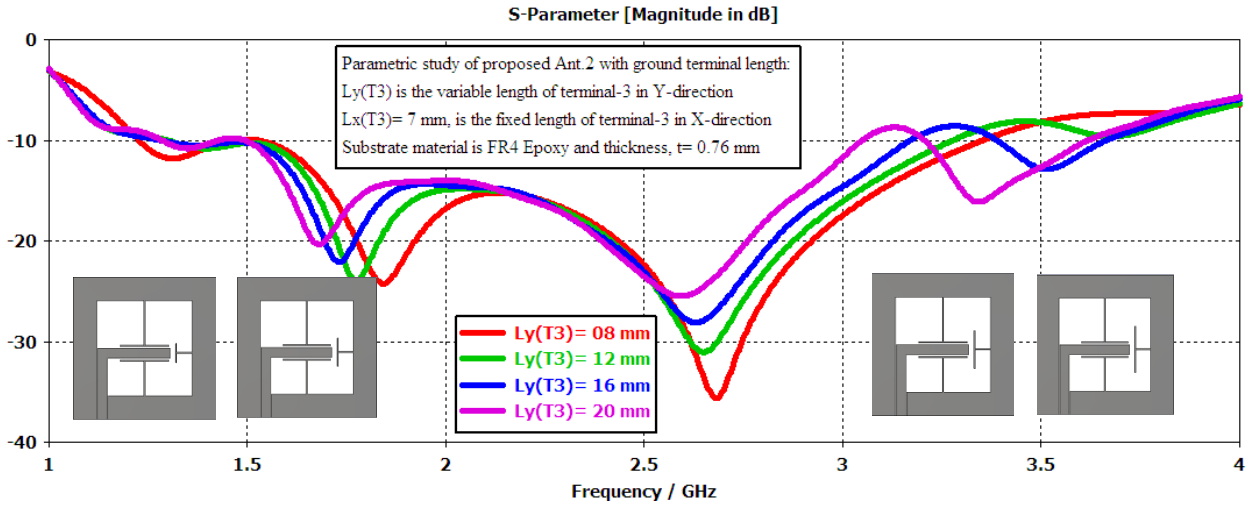

Figure 11. Parametric study ($|S_{11}|$) of proposed Ant.2 with Ly (T3) stub; 8 mm ≤ Ly (T3) ≤20 mm.

Table 4. Optimal resonance frequencies of proposed Ant.2 with different configurations.

Design Steps of Ant.2	Various Length of Ground Terminal Stubs						f_{rN} in GHz at (−dB); N = 1, 2, 3		
	Lx(T1) (mm)	Ly(T1) (mm)	Lx(T2) (mm)	Ly(T2) (mm)	Lx(T3) (mm)	Ly(T3) (mm)	f_{r1} at (−dB)	f_{r2} at (−dB)	f_{r3} at (−dB)
Step-1	20.50	19	20.50	15	1	8	1.25 (12)	1.80 (25)	2.7 (36)
Step-2	20.50	19	20.50	15	3	12	1.75 (25)	2.65 (31)	-
Step-3	20.50	19	20.50	15	5	16	1.70 (24)	2.65 (28)	3.5 (14)
Step-4	20.50	19	20.50	15	7	20	1.65 (20)	2.60 (25)	3.2 (16)

4.2. Effect of substrate materials on $|S_{11}|$ parameter of Ant.1

The effect of different substrate materials and their thicknesses on antenna performances have been investigated in this section. The resonance frequencies are dependent on the substrate area, thickness, and dielectric constant. The optimal thicknesses of substrate materials are used to evaluate $|S_{11}|$ such as 0.51 mm for Alumina, 0.76 mm for FR4, 0.95 mm for Arlon, and 1.11 mm for Rogers as tabulated in Table 5 and illustrated in Figure 12(a–d) for dual-band applications. The thickness of substrate material 0.51 mm is considered to analyze the performance of proposed Ant.1 with Arlon, FR4, Rogers, and Alumina. The characteristic with Arlon, FR4, and Rogers provides the close resonance frequencies towards higher frequency bands whereas Alumina provides resonance frequency at low-frequency bands (f_{r1} = 1.9 GHz, and f_{r2} = 2.8 GHz) as illustrated in Figure 12(a). The substrate materials thickness, t = 0.76 mm is considered to evaluate the effect of different materials on $|S_{11}|$ for dual-band applications. The characteristics of Rogers, Arlon, and FR4 are similar whereas the performance of Alumina is not significant as shown in Figure 12(b). FR4 laminated structure provides better $|S_{11}|$ as compared to Rogers and Arlon. The two resonance frequencies with FR4 are f_{r1} = 2.1 GHz and f_{r2} = 2.8 GHz for wireless applications as shown in Figure 12(b).

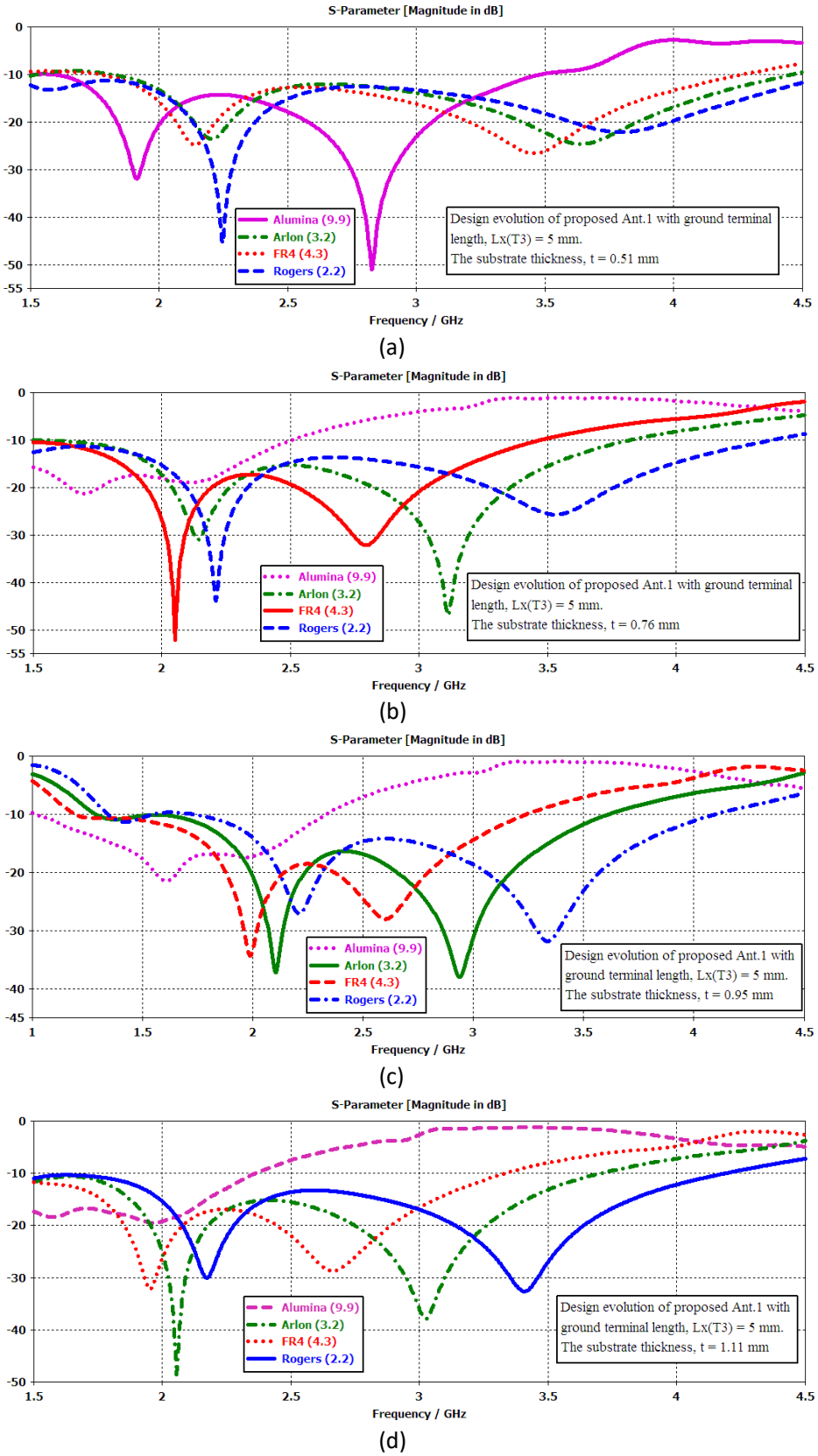

Figure 12. Parametric study ($|S_{11}|$) of proposed Ant.1 with different type of substrate materials; (a) t = 0.51mm, (b) t = 0.76 mm, (c) t = 0.95 mm, and (d) t = 1.11 mm.

Table 5. Best performance comparison of proposed Ant.1 with different substrate materials.

$\|S_{11}\|$ parameter of Ant.1 shown in Figure	Substrate Material (ε_r)	Substrate Thickness (t) (mm)	Stub Lx(T3) (mm)	Resonance Frequency (GHz)		IBW $S_{11} \leq -20$ dB (GHz)		IBW $S_{11} \leq -10$ dB (GHz)
				f_{r1}	f_{r2}	$(IBW)_1$	$(IBW)_2$	$(IBW)_{Total}$
Figure 12(a)	Alumina (9.9)	0.51	5	1.90	2.80	0.20	0.50	2.0
Figure 12(b)	FR4 (4.3)	0.76	5	2.05	2.80	0.25	0.50	2.0
Figure 12(c)	Arlon (3.2)	0.95	5	2.10	2.95	0.25	0.50	2.1
Figure 12(d)	Rogers (2.2)	1.11	5	2.20	3.40	0.15	0.55	2.5

The optimal substrate thickness of 0.95 mm Arlon (f_{r1} = 2.1 GHz, and f_{r2} = 2.95 GHz) provides a higher magnitude of the $|S_{11}|$ parameter among the four considered substrates as shown in Figure 12(c). The optimal thickness of the Rogers substrate is 1.11 mm which offers wider IBW with two resonance frequencies (f_{r1} = 2.2 GHz, and f_{r2} = 3.4 GHz), among all the considered substrates as shown in Figure 12(d).

4.3. Effects of substrate materials on $|S_{11}|$ parameter of Ant.2

The optimal thicknesses of substrate materials are taken of value 0.76 mm for triple and quad-band applications to evaluate the $|S_{11}|$ for the proposed Ant.2. The performance parameters of all the four substrate-based antennas are tabulated in Table 6 and their characteristics are presented in Figure 13(a–b). Rogers and FR4 at Ly(T3) = 8 mm provide three resonance frequencies as shown in Figure 13(a) and Table 6 for the triple-band applications. At Ly(T3) = 16 mm, Rogers showed the quad-band application, the resonance frequencies are f_{r1} = 1.4 GHz, f_{r2} = 1.9 GHz, f_{r3} = 3.2 GHz, and f_{r4} = 3.8 GHz as depicted in Figure 13(b).

4.4. Effect of substrate thickness on $|S_{11}|$ parameter of Ant.2

Figure 14 and Table 7 show the results of the analysis of the suggested Ant.2 $|S_{11}|$ parameter for various substrate thicknesses and four substrate materials. The optimal thickness (t) = 0.95 mm for quad-band applications is most suitable for the Rogers substrate-based laminated Ant.2 which offered four resonance frequencies (f_{r1} = 1.4 GHz, f_{r2} = 1.9 GHz, f_{r3} = 3.2 GHz, and f_{r4} = 3.8 GHz) as shown in Figure 14(a). For triple-band applications, Arlon substrate thickness (t) = 0.76 mm based laminated proposed Ant.2 provides the three resonance frequencies (f_{r1} = 1.8 GHz, f_{r2} = 2.9 GHz, and f_{r3} = 3.7 GHz) as shown in Figure 14(b). The $|S_{11}|$ parameters of proposed Ant.2 based on FR4 laminated at different substrate thicknesses ranging from 0.51 mm to 0.95 mm are shown in Figure 14(c). The $|S_{11}|$ parameters of the suggested Ant.2 ensured similar $|S_{11}|$ pattern for FR4 laminated case when t = 0.63, 0.76, and 0.95 mm, but the $|S_{11}|$ parameter provides a higher magnitude for t = 0.51 mm as shown in Figure 14(c). However, FR4 laminated Ant.2 at t = 0.51 mm is more suited for triple-band (f_{r1} = 1.8 GHz, f_{r2} = 3.2 GHz, and f_{r3} = 3.8 GHz) applications, see Figure 14 (c).

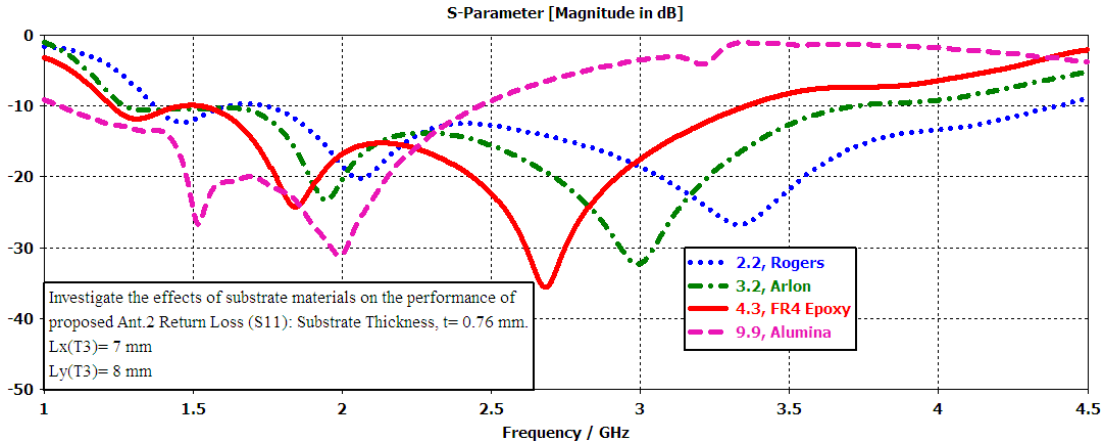

(a)

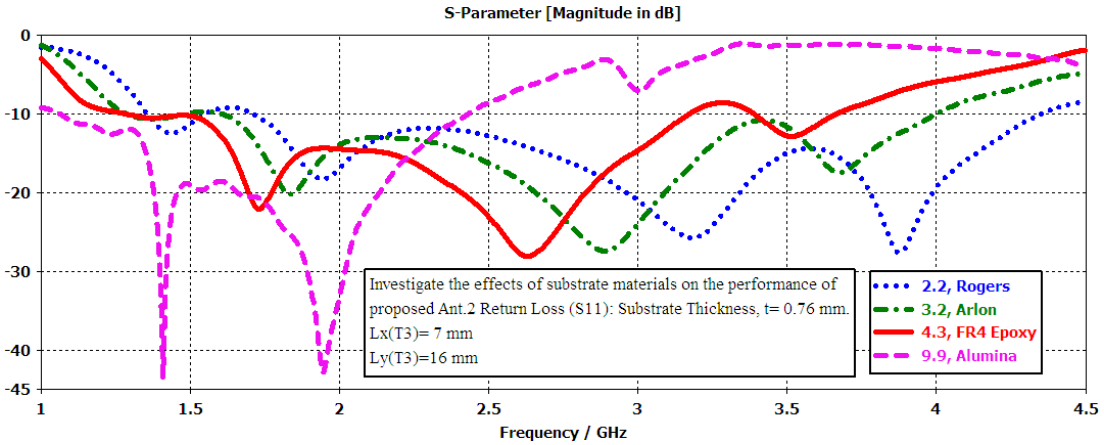

(b)

Figure 13. Parametric study ($|S_{11}|$) of proposed Ant.2 among different substrate materials by thickness (t) = 0.76 mm; (a) Ly(T3) = 8 mm, and (b) Ly(T3) = 16 mm.

Table 6. Best performance comparison of proposed Ant.2 with different substrate materials.

$\|S_{11}\|$ parameter of Ant.2	Substrate Material (ε_r)	Substrate Thickness (mm)	Stub Ly(T3) (mm)	f_{rN} in GHz (N = 1, 2, 3, 4)				IBW in GHz at (−dB)			
				f_{r1}	f_{r2}	f_{r3}	f_{r4}	$(IBW)_1$	$(IBW)_2$	$(IBW)_3$	$(IBW)_4$
Figure 13(a)	Rogers (2.2)	0.76	8	1.45	2.10	3.35	-	0.25 (10)	0.35 (15)	0.50 (20)	- -
	Arlon (3.2)			1.90	3.00	-	-	0.40 (15)	0.50 (20)	- -	- -
	FR4 (4.3)			1.30	1.80	2.65	-	0.15 (10)	0.45 (15)	0.50 (20)	- -
	Alumina (9.9)			1.50	2.00	-	-	0.17 (20)	0.45 (20)	- -	- -
Figure 13(b)	Rogers (2.2)	0.76	16	1.40	1.90	3.20	3.85	0.10 (10)	0.45 (12)	0.75 (15)	0.30 (20)
	Arlon (3.2)			1.80	2.75	3.65	-	0.35 (13)	1.00 (15)	0.50 (10)	- -
	FR4 (4.3)			1.75	2.65	3.50	-	0.25 (15)	0.40 (20)	0.25 (10)	- -
	Alumina (9.9)			1.40	1.90	-	-	0.10 (20)	0.45 (20)	- -	- -

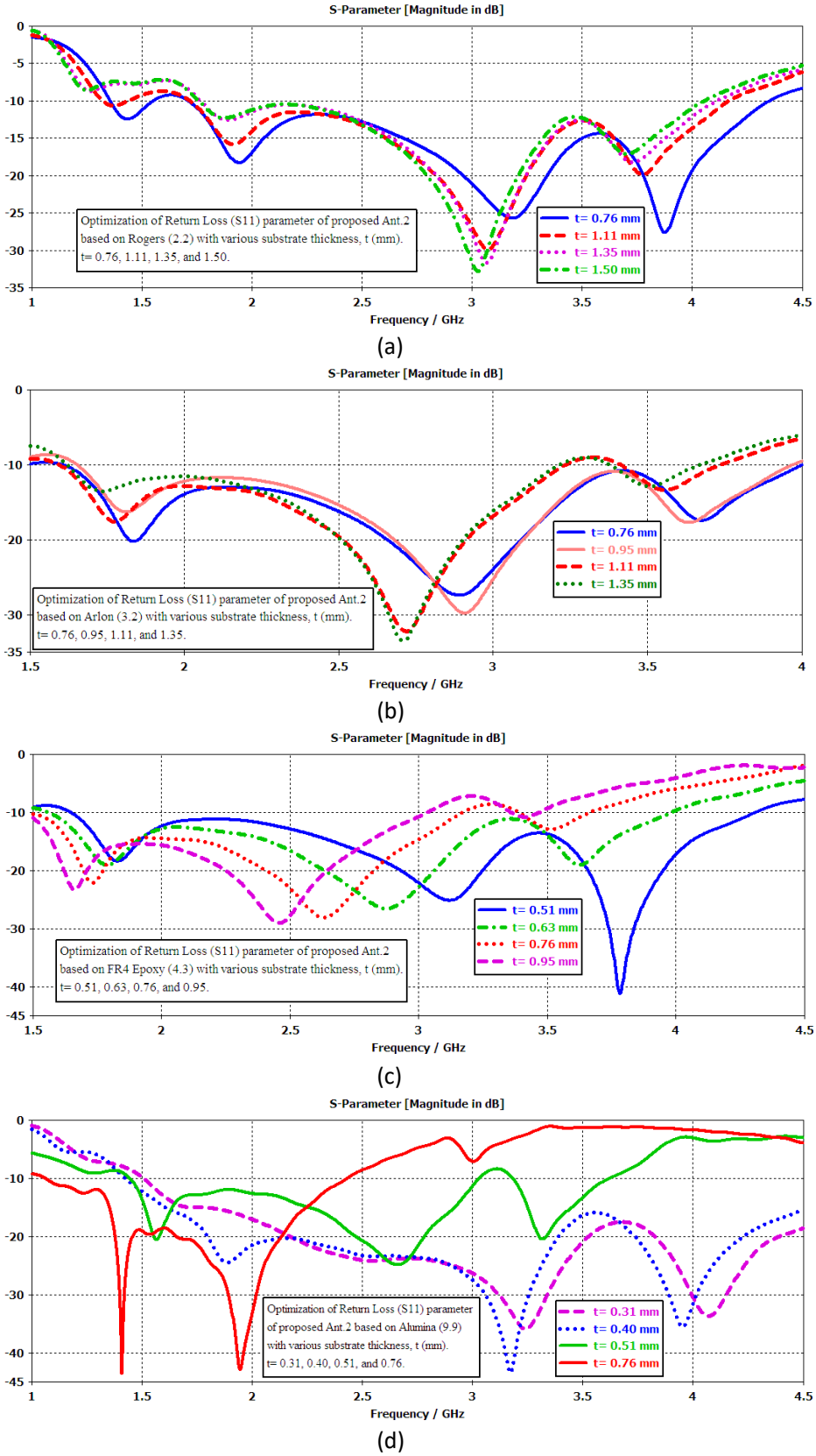

Figure 14. Parametric study ($|S_{11}|$) of proposed Ant.2 along with different substrate thicknesses; (a) Based on Rogers, (b) Based on Arlon, (c) Based on FR4, and (d) Based on Alumina.

Table 7. Best performance comparison of proposed Ant.2 with different substrate thicknesses.

$\|S_{11}\|$ parameter of Ant.2 shown in Figure	Substrate Material (ε_r)	Substrate Thickness (t, mm)	f_{rN} in GHz, (N = 1, 2, 3, 4)			
			f_{r1}	f_{r2}	f_{r3}	f_{r4}
Figure 14(a)	Rogers (2.2)	0.95	1.40	1.90	3.20	3.85
		1.11	1.35	1.90	3.10	3.80
		1.35	-	1.85	3.10	3.75
		1.50	-	1.85	3.05	3.75
Figure 14(b)	Arlon (3.2)	0.76	1.80	2.90	3.75	-
		0.95	1.78	2.90	3.70	-
		1.11	1.75	2.77	3.55	-
		1.35	1.65	2.75	3.50	-
Figure 14(c)	FR4 (4.3)	0.51	1.85	3.15	3.80	-
		0.63	1.80	2.90	3.65	-
		0.76	1.75	2.65	3.50	-
		0.95	1.65	2.45	3.40	-
Figure 14(d)	Alumina (9.9)	0.31	-	3.25	4.10	-
		0.40	1.90	3.20	3.95	-
		0.51	1.60	2.65	3.35	-
		0.76	1.402	1.95	-	-

The optimal thickness t = 0.40 mm of Alumina substrate is considered to ensure higher frequency triple-band applicability resonating at f_{r1} = 1.9 GHz, f_{r2} = 3.2 GHz, and f_{r3} = 3.9 GHz. The thickness t = 0.76 mm was taken to achieve lower frequency dual-band (f_{r1} = 1.4 GHz, and f_{r2} = 1.9 GHz) applications for proposed Ant.2 as shown in Figure 14(d).

Figure 15 shows the optimal values ($|S_{11}|$) of proposed Ant.1 and Ant.2, which are listed in Table 8. The Ant.1 is investigated for dual-band applications on various substrate materials. The obtained results show that resonance frequencies are shifted towered the lower frequencies range at a higher dielectric constant and low substrate thickness as shown in Figure 15(a). As illustrated in Figure 15(b) and listed in Table 8, the proposed Ant.2 can be used for triple and quad-band applications ranging from 1.35 to 4.25 GHz ($S_{11} \leq -10$ dB).

Table 8. Excellent performance of proposed antennas along with four dielectric materials.

Resonance Frequencies (f_r) of Proposed Ant.1 and Ant.2										
Laminated Antenna (ε_r)	Proposed Ant.1				Proposed Ant.2					
	t (mm)	f_{r1} (GHz)	f_{r2} (GHz)	Response	t (mm)	f_{r1} (GHz)	f_{r2} (GHz)	f_{r3} (GHz)	f_{r4} (GHz)	Response
Rogers (2.2)	1.11	2.15	3.40	Dual-band	0.95	1.40	1.90	3.20	3.80	Quad-band
Arlon (3.2)	0.95	2.10	2.90	Dual-band	0.76	-	1.80	2.85	3.65	Triple-band
FR4 (4.3)	0.76	2.05	2.80	Dual-band	0.51	-	1.80	3.10	3.75	Triple-band
Alumina (9.9)	0.51	1.90	2.80	Dual-band	0.40	-	1.85	3.15	3.95	Triple-band

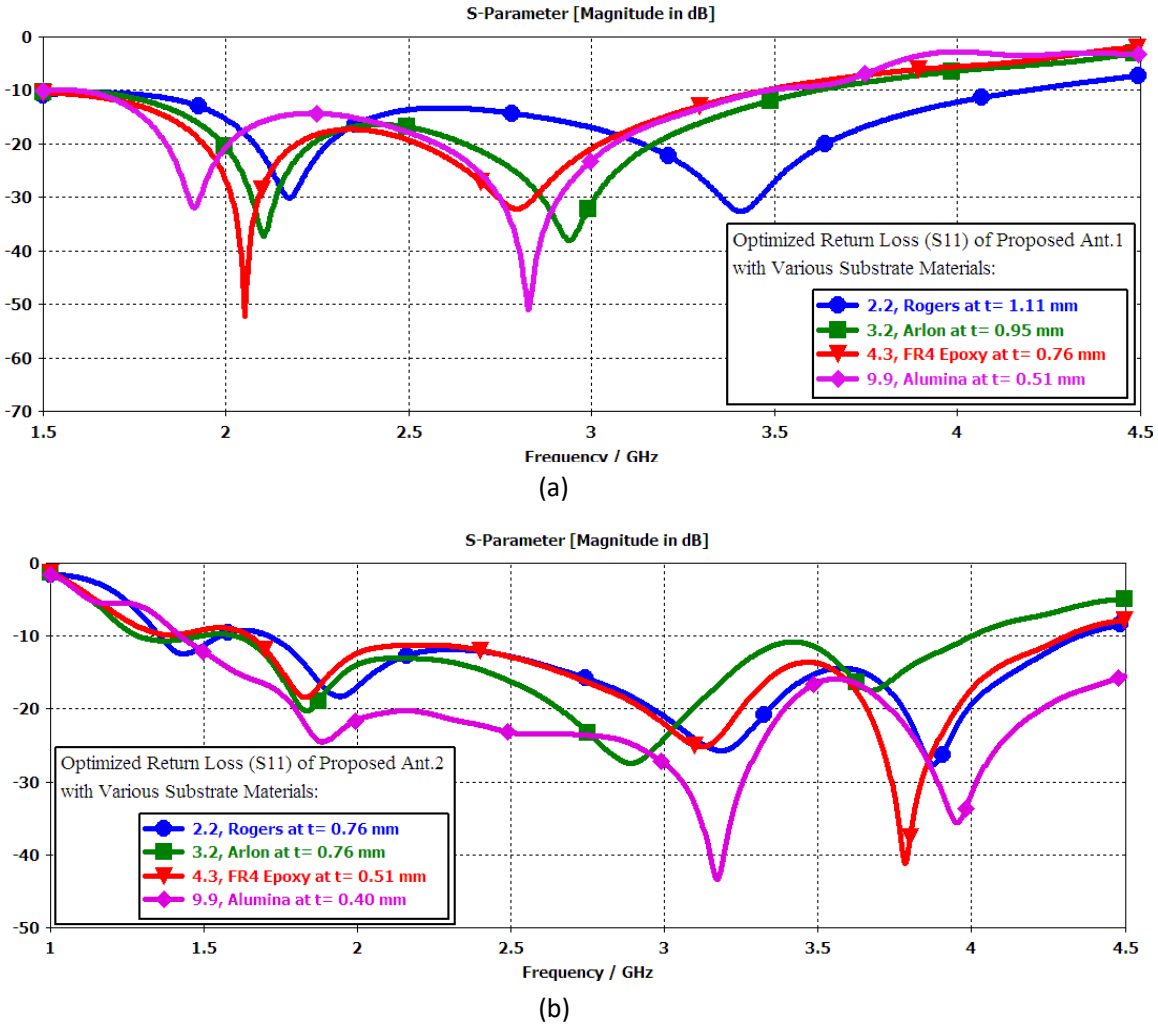

Figure 15. Optimized $|S_{11}|$ along with substrate material and its finest thickness; (a) Relative results of proposed Ant.1, and (b) Relative results of proposed Ant.2.

5. Results and discussion

The simulation and measurement results of a CPW-fed Ant.2 (Q) with several resonance frequencies and bands are described in this section. The suggested multi-ground terminal resonator stubs printed CPW-fed antennas were constructed on FR4 substrate using standard photolithographic method after optimization in CST Microwave Studio as shown in Figure 16 (a). The proposed antenna's return loss ($|S_{11}|$) was measured on Keysight Technologies (N5224B) network analyzer for the validation of the simulated result. The radiation pattern of antenna is measured inside the near-field anechoic chamber as shown Figure 16 (b).

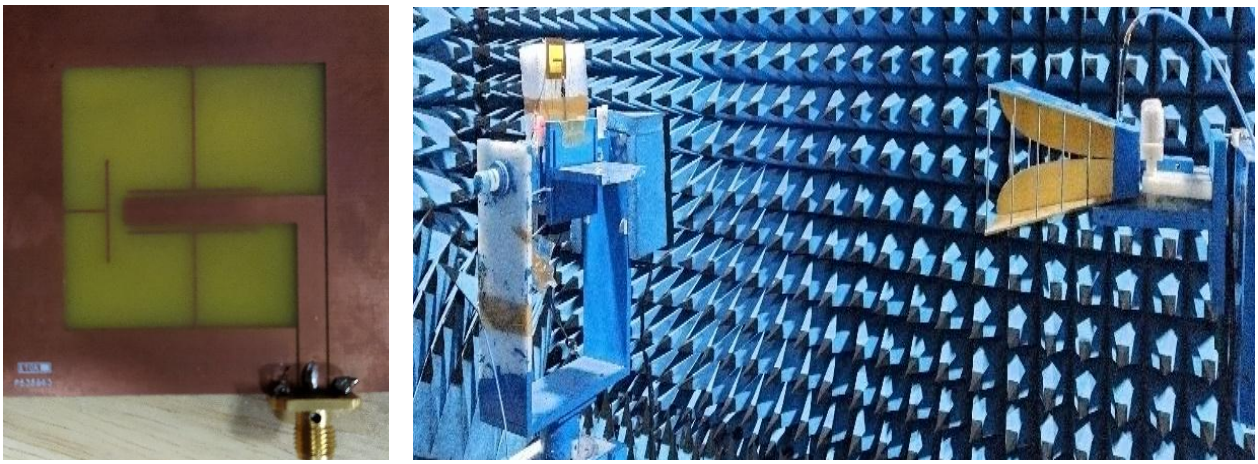

(a) (b)

Figure 16. Photograph of the proposed Ant.2 based on FR4 substrate; (a) Front view of antenna Prototype, and (b) Antenna inside anechoic chamber.

Figure 17 (a-b) shows the simulated and measured $|S_{11}|$ and Voltage Standing Wave Ratio (VSWR) vs frequency plots of the proposed antenna. As can be seen in Figure 17 (a), there is a good agreement between simulated and measured results with some predictable inconsistencies due to fabrication tolerance and measurement environments, which confirms the theoretical prediction. The fabricated antenna is resonating at 1.75/2.75/3.50 GHz frequencies and cover three separate impedance bandwidths of 0.25 GHz at −15 dB, 0.40 GHz at −20 dB, and 0.25 GHz at −10 dB, with respect to the appropriate resonant frequencies at $|S_{11}| \leq -10$ dB level, which can satisfy both the PCS 1.8/1.9 GHz (1.750-1.870 GHz and 1.880-1.990 GHz), and WiMAX 2.5/3.5 GHz (2.500-2.690 GHz and 3.400-3.690 GHz) bands. Figure 17 (b) shows that the simulated and measured VSWR values are in good agreement, with minor expected variations due to variations in actual values of relative permittivity, loss tangent (tan δ) and thickness of the material taken for measurement and simulation, fabrication error, soldering of the SMA connector with the antenna and measurement environment, confirming the theoretical prediction.

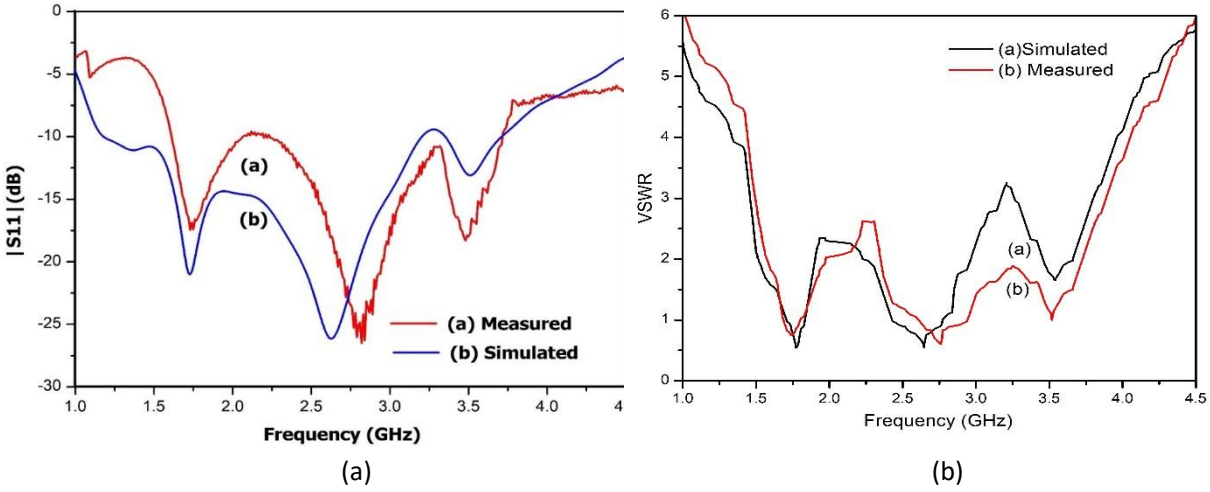

(a) (b)

Figure 17. Simulated and measured result of the proposed Ant.2; (a) Return loss ($|S_{11}|$), and (b) VSWR.

The measurement setup of radiation pattern and gain is carried out using broadband LB-10180-NF horn antenna as reference antenna in an anechoic chamber of the developed prototype antenna. Figure 18 depicts the measured E-plane and H-plane radiation patterns of a CPW-fed Ant.2 with three resonance frequencies of values 1.75, 2.65, and 3.50 GHz. Figure 18 (a) illustrations the far-field patterns of co-polarization in the E-plane ($\phi = 0$) and H-plane ($\phi = 90$), respectively. It could be seen that antenna has almost omnidirectional co-polarized patterns at $\phi = 0°$ angle and nearly bi-directional co-polarized patterns at $\phi = 90°$ angle at the resonance frequency of 3.5 GHz for WiMAX band in H-plane.

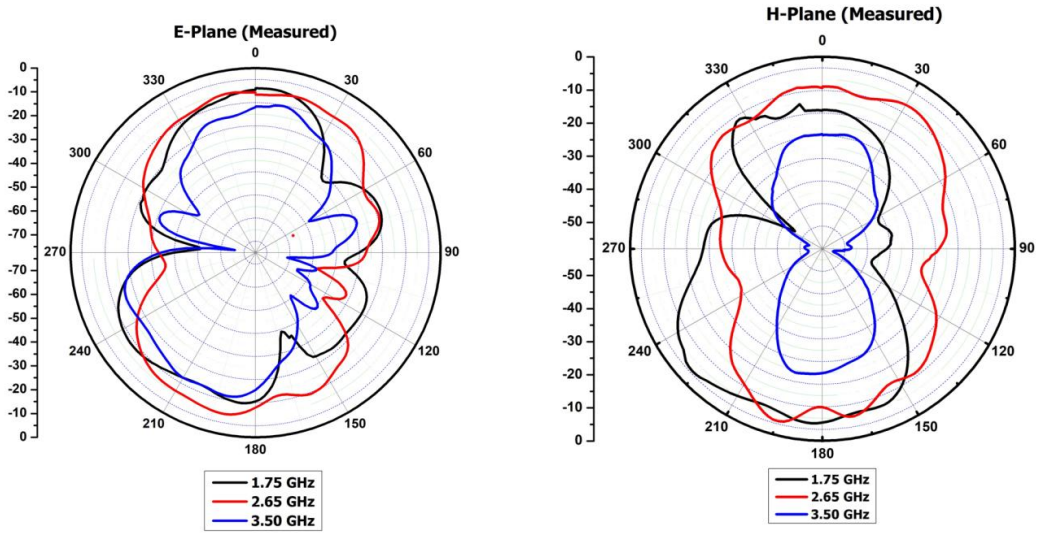

(a)

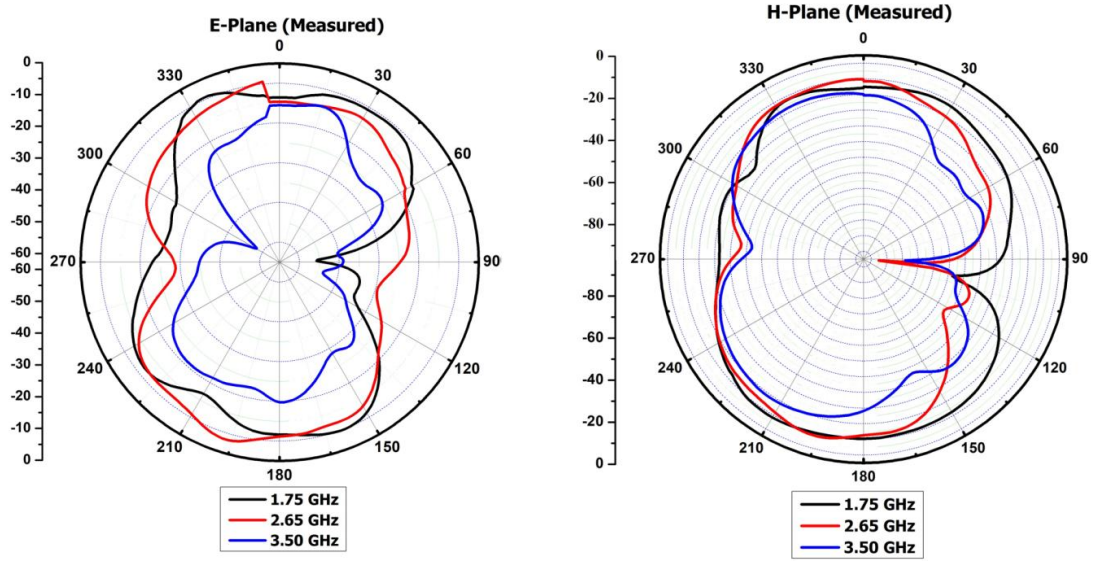

(b)

Figure 18. Measured radiation patterns of proposed Ant.2 at three resonance frequencies; (a) Co-polarization E/H-plane, and (b) Cross-polarization E/H-plane.

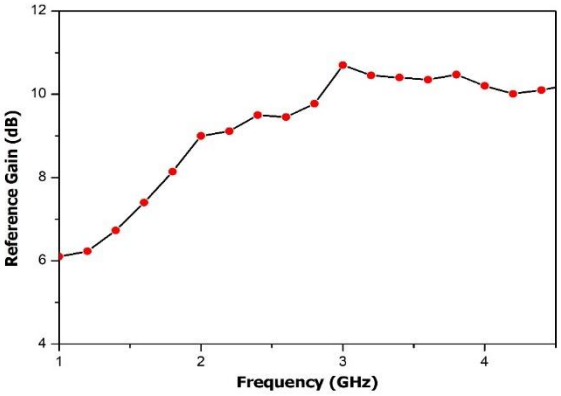

Figure 19. Reference gain (dB) against frequency of the proposed Ant.2.

Figure 18 (b) illustrates that the cross-polarization patterns of the antenna are fairly improved at the same resonance frequencies as compared to co-polarization patterns in E-plane and H-plane, respectively. At 1.75 and 2.65 GHz frequencies, the proposed Ant.2 has omnidirectional radiation patterns in the both (E/H)-plane, while the radiation patterns at 3.5 GHz have slightly departed from omnidirectional radiation patterns due to asymmetrical structure of antenna. Figure 19 depicts the measured reference gain of the proposed Ant.2 as a function of frequency. The reference gain variation is 7.25-10.15 dB of proposed structure. At the resonance frequencies of 1.75, 2.75, and 3.50 GHz, the reference gain of antenna is 7.25, 9.75, and 10.15 dB, respectively as shown in Figure 19.

Table 9 presents the performance comparison of proposed antennas (Ant.1 and Ant.2) with some of the previously reported antennas referred in [6–16] which utilized the same dielectric substrate for the fair comparison.

Although the overall area of the proposed antennas is identical to the reported antennas, its bandwidth is larger than all the works mentioned in Table 9. In terms of IBW, the proposed structure is performing far better than the existing structures except for the structures proposed in [10], [12], and [15]. However, as the major goal of this research is to increase the number of bands with a wide bandwidth, the proposed topology accomplishes its goal.

6. Conclusions

The performance of the antenna in terms of $|S_{11}|$ characteristics are investigated for four different substrate materials at a different thickness in this article. The designs of two antennas are proposed, and their performances are analyzed for dual, triple, and quad-band applications. The multi resonating modes frequencies of proposed Ant.1 and Ant.2 can be obtained by optimal selection of the dielectric substrate materials, their thicknesses, and the length of the three-ground terminal stub resonators. The proposed Ant.1 is expected to be useful in wide-band services of PCS-1900 (1.880-1.990 GHz), GSM-1900 (1.850-1.990 GHz), IMT-2000 (1.920-2.170 GHz), UMTS (1.900-2.170 GHz), IMT-2800 (2.700-2.900 GHz), and WiMAX (3.200-3.800 GHz) for dual-band applications. The proposed Ant.2 is designed for receiving ability for IMT service (f_c = 1.4 GHz, FDD LTE band), GSM-1800 (1.710-1.805 GHz), GSM-1900 (1.850-1.990 GHz), IMT-2800 (2.700-2.900 GHz), Radiolocation Service (f_c = 3.1 GHz), and IMT-3800 (3.400-4.200 GHz) for triple and quad-band applications. The achieved $|S_{11}|$ results of proposed antennas (Ant.1 and Ant.2) demonstrate that fundamental resonance frequencies are moved towards the low-frequency band at a higher dielectric constant and low substrate thickness. Thus, substrate of high dielectric constant ensures antenna miniaturization. Due to the low

profile, simple structure, and broadband impedance characteristics, the proposed antennas can suitably be employed for several wideband RF communications.

Table 9. Performance comparison of the proposed antennas with other reported antennas.

[Ref.] Year	Substrate Material (ε_r)	t (mm)	Size (mm^2)	f_{rN} in GHz (N=1, 2, 3, 4) f_{r1}	f_{r2}	f_{r3}	f_{r4}	IBW in GHz at ≤ −10 dB $(IBW_1)_{-dB}$	$(IBW_2)_{-dB}$	$(IBW_3)_{-dB}$	$(IBW_4)_{-dB}$
[06] 2006	FR4 (4.4)	0.80	120×40	2.45	5.45	-	-	(0.51) $_{-10\ dB}$	(1.01) $_{-10\ dB}$	-	-
[07] 2010	Rogers (2.2)	2.00	64×62	2.44	3.55	-	-	(0.11) $_{-10\ dB}$	(0.14) $_{-10\ dB}$	(0.63) $_{-10\ dB}$	-
[08] 2015	Rogers (2.33)	3.20	40×28	2.45	3.50	5.28	-	(0.14) $_{-10\ dB}$	(0.15) $_{-10\ dB}$	(0.24) $_{-10\ dB}$	-
[09] 2018	FR4 (4.2)	1.60	70×70	2.31	2.40	2.48	-	(0.05) $_{-10\ dB}$	(0.06) $_{-10\ dB}$	(0.06) $_{-10\ dB}$	-
[10] 2019	FR4 (4.2)	0.80	30×28	2.62	3.55	5.56	-	(0.25) $_{-10\ dB}$	(0.48) $_{-10\ dB}$	(0.50) $_{-20\ dB}$	-
[11] 2019	FR4 (4.4)	1.60	65×30	2.45	5.15	-	-	(0.45) $_{-10\ dB}$	(0.45) $_{-10\ dB}$		-
[12] 2020	FR4 (4.3)	1.60	50×50	2.45	3.80	5.80	-	(0.08) $_{-10\ dB}$	(0.95) $_{-20\ dB}$	(1.20) $_{-20dB}$	-
[13] 2020	Rogers (10.2)	1.27	25×31	2.46	5.11	-	-	(0.11) $_{-10\ dB}$	(0.07) $_{-10\ dB}$	-	-
[14] 2021	Rogers (3.0)	0.80	40×60	1.64	1.79	2.11	2.43	(0.04) $_{-10\ dB}$	(0.10) $_{-10\ dB}$	(0.07) $_{-10\ dB}$	(0.08) $_{-10dB}$
	Duroid (2.2)	1.60		1.75	1.87	2.24	-	(0.07) $_{-5\ dB}$	(0.06) $_{-5\ dB}$	(0.05) $_{-5\ dB}$	-
	FR4 (4.4)	1.60		1.63	1.80	2.31	-	(0.11) $_{-10\ dB}$	(0.09) $_{-10\ dB}$	(0.07) $_{-10\ dB}$	-
[15] 2021	FR4 (4.4)	0.80	50×50	2.50	3.60	6.00	-	(0.20) $_{-16\ dB}$	(0.90) $_{-20\ dB}$	(0.30) $_{-20\ dB}$	-
[16] 2021	FR4 (4.4)	1.60	116×116	1.02	1.75	-	-	(0.35) $_{-15\ dB}$	(0.38) $_{-12\ dB}$	-	-
Proposed Ant.1	Rogers (2.2)	1.11	50×50	2.15	3.40	-	-	(0.70) $_{-10\ dB}$	(0.75) $_{-10\ dB}$	-	-
	Arlon (3.2)	0.95		2.10	2.90	-	-	(0.40) $_{-10\ dB}$	(0.55) $_{-20\ dB}$	-	-
	FR4 (4.3)	0.76		2.05	2.80	-	-	(0.45) $_{-10\ dB}$	(0.50) $_{-20\ dB}$	-	-
	Alumina (9.9)	0.51		1.90	2.80	-	-	(0.55) $_{-15\ dB}$	(0.60) $_{-20\ dB}$	-	-
Proposed Ant.2	Rogers (2.2)	0.95	50×50	1.40	1.90	3.20	3.80	(0.25) $_{-10\ dB}$	(0.50) $_{-12\ dB}$	(0.75) $_{-15\ dB}$	(0.55) $_{-15dB}$
	FR4 (4.3)	0.51		-	1.80	3.10	3.75	-	(0.35) $_{-12\ dB}$	(0.70) $_{-15\ dB}$	(0.65) $_{-10dB}$

Acknowledgments

The authors would like to acknowledge and convey their sincere thanks to Prof. Binod Kumar Kanaujia, of National Institute of Technology (NIT), Jalandhar, Punjab, India, and B. R. Ambedkar Engineering College, Geeta Nagar, Delhi for providing necessary facilities of measurement lab to complete this research work.

Conflict of interest

The authors declare that they have no conflict of interest regarding this paper.

References

1. Blostein SD, Leib H (2003) Multiple antenna systems: their role and impact in future wireless access. *IEEE Commun Mag* 41: 94–101. https://doi.org/10.1109/MCOM.2003.1215645
2. Li X, Shi XW, Hu W, et al. (2013) Compact Triband ACS-Fed Monopole Antenna Employing Open-Ended Slots for Wireless Communication. *IEEE Antenn Wirel Pr* 12: 388–391. https://doi.org/10.1109/LAWP.2013.2252414
3. Chen H, Yang X, Yin YZ, et al. (2013) Triband Planar Monopole Antenna with Compact Radiator for WLAN/WiMAX Applications. *IEEE Antenn Wirel Pr* 2: 1440–1443. https://doi.org/10.1109/LAWP.2013.2287312
4. Peng CM, Chen IF, Yeh JW (2013) Printed Broadband Asymmetric Dual-Loop Antenna for WLAN/ Wi-MAX Applications. *IEEE Antenn Wirel Pr* 12: 898–901. https://doi.org/10.1109/LAWP.2013.2273231
5. Dang L, Lei ZY, Xie YJ, et al. (2010) A Compact Microstrip Slot Triple-Band Antenna for WLAN/WiMAX Applications. *IEEE Antenn Wirel Pr* 9: 1178–1181. https://doi.org/10.1109/LAWP.2010.2098433
6. Wu CM, Chiu CN, Hsu CK (2006) A new non-uniform meandered and fork-type grounded antenna for triple-band WLAN applications. *IEEE Antenn Wirel Pr* 5: 346–348. https://doi.org/10.1109/LAWP.2006.880692
7. Peng L, Ruan C, Wu X (2010) Design and Operation of Dual/Triple-Band Asymmetric M-Shaped Microstrip Patch Antennas. *IEEE Antenn Wirel Pr* 9: 1069–1072. https://doi.org/10.1109/LAWP.2010.2091671
8. Reddy BR, Vakula D (2015) Compact Zigzag-Shaped-Slit Microstrip Antenna with Circular Defected Ground Structure for Wireless Applications. *IEEE Antenn Wirel Pr* 14: 678–681. https://doi.org/10.1109/LAWP.2014.2376984
9. Dabas T, Kanaujia BK, Gangwar D, et al. (2018) Design of multiband multi-polarised single feed patch antenna. *IET Microw Antenna P* 12: 2372–2378. https://doi.org/10.1049/iet-map.2018.5401
10. Manouare AZ, Ibnyaich S, Seetharamdoo D, et al. (2019) Design, Fabrication and Measurement of a Novel Compact Triband CPW-Fed Planar Monopole Antenna Using Multi-type Slots for Wireless Communication Applications. *J Circuit Syst Comp* 29: 1–23. https://doi.org/10.1142/S0218126620500322
11. Singla G, Khanna R, Parkash D (2019) CPW fed rectangular rings-based patch antenna with DGS for WLAN/UNII applications. *Int J Microw Wirel T* 11: 523–531. https://doi.org/10.1017/S1759078719000023

12. Yassini AE, Ibnyaich S, Chabaa S, et al. (2020) Miniaturized broadband multiband planar antenna with a symmetric quarter circular ground plane for WLAN/WiMAX standards. *Microw Opt Techn Let* 10: 1–12. https://doi.org/10.1002/mop.32402
13. Bendahmane Z, Ferouani S, Sayah C (2020) High Permittivity Substrate and DGS Technique for Dual-Band Star-Shape Slotted Microstrip Patch Antenna Miniaturization. *Progress In Electromagnetics Research C* 102: 163–174. https://doi.org/10.2528/PIERC20021501
14. Ansal KA, Kumar AS, Baby SM (2021) Comparative analysis of CPW fed antenna with different substrate material with varying thickness. *Materials Today: Proceedings* 37: 257–264. https://doi.org/10.1016/j.matpr.2020.05.201
15. Fu Q, Feng Q, Chen H (2021) Design and Optimization of CPW-Fed Broadband Circularly Polarized Antenna for Multiple Communication Systems. *Progress In Electromagnetics Research Letters* 99: 65–74. https://doi.org/10.2528/PIERL21062205
16. Ma R, Feng Q (2021) Design of Broadband Circularly Polarized Square Slot Antenna for UHF RFID Applications. *Progress In Electromagnetics Research C* 111: 97–108. https://doi.org/10.2528/PIERC21021403
17. Singh SK, Sharan T, Singh AK (2020) A comparative performance analysis of various shapes and substrate materials loaded coplanar waveguide-fed antennas. *Materials Today: Proceedings* 34: 643–648. https://doi.org/10.1016/j.matpr.2020.03.133
18. Singh SK, Sharan T, Singh AK (2021) Miniaturization of CPW-Fed Patch Antenna by Using Dielectric Materials for 2.4 GHz (WLAN/ISM) Applications. *Macromolecular Symposia* 397: 1–10. https://doi.org/10.1002/masy.202100008
19. Dejen A, Jayasinghe J, Ridwan M, et al. (2022) Genetically engineered tri-band microstrip antenna with improved directivity for mm-wave wireless application. *AIMS Electronics and Electrical Engineering* 6: 1–15. https://doi.org/10.3934/electreng.2022001
20. Ullah MH, Islam MT, Mandeep JS (2013) A parametric study of high dielectric material substrate for small antenna design. *Int J Appl Electrom* 41: 193–198. https://doi.org/10.3233/JAE-2012-1603
21. Raveendran A, Sebastian MT, Raman S (2019) Applications of Microwave Materials: A Review. *J Electron Mater* 48: 2601–2634. https://doi.org/10.1007/s11664-019-07049-1
22. Fechine PBA, Tavora A, Kretly LC, et al. (2006) Microstrip antenna on a high dielectric constant substrate: $BaTiO_3$ (BTO)-$CaCu_3Ti_4O_{12}$(CCTO) composite screen-printed thick films. *J Electron Mater* 35: 1848–1856. https://doi.org/10.1007/s11664-006-0167-0
23. Toma RN, Shohagh IA, Hasan MN (2019) Analysis of the effect of Changing Height of Substrate of Square Shaped Microstrip Patch Antenna on the Performance for 5G Application. *Int J Microw Wirel T* 9: 33–45. https://doi.org/10.5815/ijwmt.2019.03.04
24. Kumar A, Jhanwar D, Sharma MM (2017) A compact printed multistubs loaded resonator rectangular monopole antenna design for multiband wireless systems. *Int J RF Microw C E* 27: 1–10. https://doi.org/10.1002/mmce.21147
25. Sharma MM, Deegwal JK, Govil MC, et al. (2015) Compact printed ultra-wideband antenna with two notched stop bands for WiMAX and WLAN. *Int J Appl Electrom* 47: 523–532. https://doi.org/10.3233/JAE-140007

AIMS Press